Red Nacional de
Investigadores
en Economía

It Takes Two to Tango, but More to Assess Systemic Risk: Credit Networks Through the Lens of Hypergraphs

Federico Forte (BBVA Research)

DOCUMENTO DE TRABAJO N° 406

Septiembre de 2026

Citar como:
Forte, Federico (2026). It Takes Two to Tango, but More to Assess Systemic Risk: Credit Networks Through the Lens of Hypergraphs Documento de trabajo RedNIE N°406.

It Takes Two to Tango, but More to Assess Systemic Risk: Credit Networks Through the Lens of Hypergraphs

Federico D. Forte*

August 2026

Abstract

This paper introduces a higher-order network framework based on hypergraphs for assessing systemic risk in bank-firm credit relationships. Unlike conventional network approaches, which rely on pairwise connections, hypergraphs explicitly represent groups of financial institutions jointly exposed to the same borrower as a multilateral interaction. We compare traditional centrality metrics with hypergraph-specific measures to identify systemically important financial institutions, applying these techniques empirically to credit registry data from the Central Bank of Argentina. An adjusted version of the H-eigenvector centrality measure is also proposed, which nonlinearly combines each creditor's lending amount with the centrality of its co-lenders participating in the same higher-order interactions. We then assess the systemic impact associated with distress shocks to the top-ranked entities selected by each metric. The proposed hypergraph-based measure consistently identifies sets of institutions whose distress generates greater amplified systemic impact than those selected by traditional centrality measures. To the best of our knowledge, this paper provides the first application of hypergraphs to modern bank-firm credit networks for systemic risk assessment. The results show that explicitly accounting for higher-order interactions reveals dimensions of systemic relevance not fully captured by dyadic metrics, providing financial supervisors with a complementary tool for identifying systemically important institutions. This framework can also be readily applied to different countries and financial systems.

JEL Classification: D85, G21, G28, C63.

Keywords: Systemic risk, Hypergraphs, Financial institutions, Credit networks, Financial stability.

* Present affiliation: BBVA Research, Banco BBVA Argentina. The views expressed in this publication are those of the author and do not necessarily reflect the position of BBVA. E-mail: federico.forte@bbva.com.

1. Introduction

Credit relationships constitute one of the fundamental pillars of financial systems. They are the core activity of banks and usually account for the largest share of their assets. At the same time, credit is one of the main drivers of firms' investment and growth, and consequently of economic activity in general. For this reason, relationships between banks and firms represent one of the most relevant forms of economic interconnectedness underlying the allocation and mobilization of resources in modern economies (De Masi & Gallegati, 2012; Wang et al., 2025).

Among the approaches used to characterize these relationships, complex network theory has gained prominence as a tool for disentangling the structural features of intertwined financial linkages (Acemoglu et al., 2015). Within this framework, credit networks have traditionally been represented as bipartite networks connecting banks and firms (Marotta et al., 2015; Miranda & Tabak, 2013; Straka et al., 2018), or through one-mode projections of those bipartite structures, linking institutions according to their shared connections (for example, two banks may be linked when they are jointly exposed to the same borrowing firms, as in De Masi et al., 2011). More recently, this literature has been extended to multilayer settings, in order to incorporate several layers of connectivity rather than a single type of interlinkage (Cao et al., 2021; Lei et al., 2025; Wang et al., 2025), enabling a more comprehensive examination of multiple transmission channels. Nevertheless, these approaches remain based on *dyadic* representations of credit relationships and therefore do not explicitly account for the *multilateral* interdependencies that arise when several financial institutions are simultaneously exposed to the same borrower. Although the underlying loan contracts are bilateral, borrower distress may affect all creditor institutions simultaneously, while credit retrenchment by one lender may impair a firm's capacity to service its obligations to the others.

When a firm receives loans from multiple banks at the same time, the traditional network representation has modeled these relationships as a set of bilateral connections (De Masi & Gallegati, 2012; Fujiwara et al., 2009). Nevertheless, the co-financing of a single agent by multiple financial institutions actually generates a simultaneous multilateral relationship of shared exposure among several entities, rather than simply the sum of bilateral connections between them. Thus far, most empirical analyses of financial networks have focused on relationships between pairs of agents, and graphs have proven to be a suitable tool for examining the topological structure of such interactions (Barabási, 2016; Newman, 2010). However, a nascent and growing body of literature argues that, in many empirical settings, it is more appropriate to incorporate interrelations involving more than two agents, which may connect three, four, or more agents simultaneously (for example, Battiston et al., 2020; Bianconi, 2021; Kovalenko et al., 2022). These are referred to as *higher-order interactions*, and *hypergraphs* constitute one of the main analytical frameworks used to represent them (Figure 1).

Hypergraphs generalize standard graphs by allowing multilateral connections, known as *hyperedges* or *hyperlinks*. This framework makes it possible, for example, to compute nonlinear centrality operators and account for higher-order amplification mechanisms. To date, this approach has been applied to academic collaboration networks (Patania et al., 2017), biochemical networks (Traversa et al., 2023), and social networks (Iacopini et al., 2024), among other fields. But its application to financial topics remains very limited, with only a few related studies addressing stock-price prediction (Fang et al., 2025; Han et al., 2023), stress testing in financial markets (Akgüller & Balcı, 2026) and intermediaries' substitutability in the sterling money market in 1906 (Accominotti et al., 2023).

This paper provides, to the best of our knowledge, the first application of hypergraphs to the analysis of modern bank-firm credit networks for systemic risk assessment. They offer a natural representation of the underlying structure of multilateral relationships arising from common borrower exposures among financial institutions. Reducing these inherently collective structures to collections of bilateral ties may obscure nonlinear amplification mechanisms that emerge from the joint involvement of multiple institutions in the same credit relationships. We therefore argue that examining credit networks through the lens of hypergraphs can reveal patterns and systemic effects that cannot be fully captured by simpler dyadic representations. We apply this higher-order framework empirically to a rich credit-registry dataset from Argentina, covering the period from August 2023 to December 2025.

Figure 1. Illustrative example of a bipartite network and its associated hypergraph

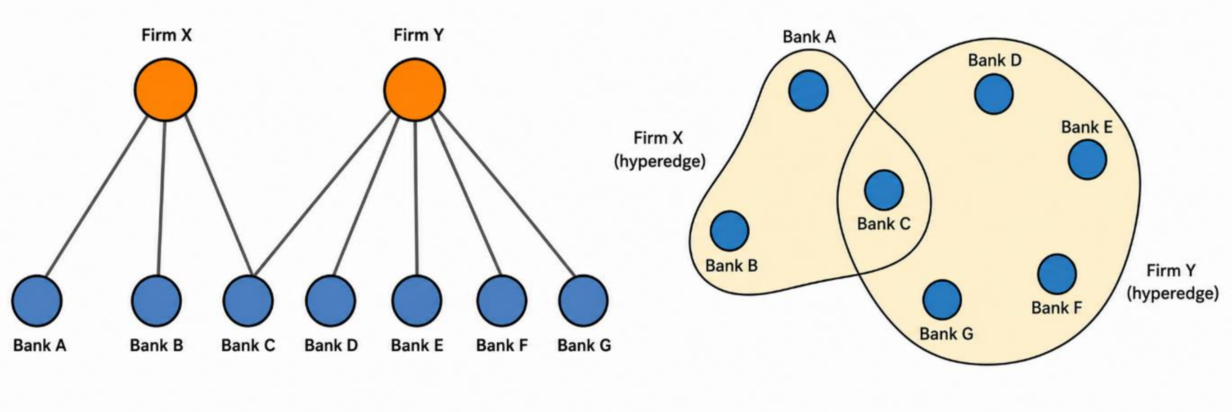

Notes: Left: illustrative example of a bipartite credit network between banks and firms. Right: hypergraph associated with the original bipartite network.

In the specific case of credit networks, when multiple banks lend to the same firm, they are jointly exposed to the same counterparty risk. A firm's default or repayment difficulties would therefore generate simultaneous stress for all its lending institutions. Conversely, systemic stress may also propagate through firms' rollover risk. If a bank faces liquidity constraints and curtails credit to its borrowers, these firms may encounter difficulties in meeting their obligations to other lending banks, thereby amplifying the initial shock and potentially giving rise to iterative spillovers across the financial system. This type of systemic risk is particularly relevant in commercial credit markets, where exposures are typically larger and more concentrated than in retail segments. For this reason, this paper focuses on commercial credit rather than on individual or retail consumer loans.

A central objective of banking regulation and supervision is the identification of systemically important institutions, whose failure or distress could generate risks for the rest of the financial system (BCBS, 2024). Regulators around the world have incorporated concepts from complex network analysis to detect such central entities, commonly described as "too-big-to-fail" or "too-interconnected-to-fail" institutions (Acemoglu et al., 2015; Acharya et al., 2017; Haldane, 2009; Hüser, 2015). Once identified, these institutions are usually subject to differentiated regulatory treatment aimed at reducing the probability and potential costs of systemic financial crises.

Multiple centrality measures have been proposed to identify systemically relevant agents in different types of networks (for an extensive review, see Chun et al., 2025). However, this field remains comparatively less developed in the context of hypergraphs. This paper attempts to contribute to filling this gap by applying centrality measures that explicitly incorporate multilateral interrelations, represented as hyperedges, and comparing their results with those obtained from more traditional graph-based metrics. In addition, we propose an adjustment to an existing hypergraph centrality measure designed to better capture specific features of financial credit networks. This new adjusted measure seeks to assess the relevance of financial institutions by combining two dimensions: their lending volume within the system and the centrality of their neighbors, while accounting for the nonlinearities inherent in multilateral interactions.

To evaluate the implications of alternative centrality measures, we estimate the systemic impact associated with the distress of the most central financial institutions identified by each of eleven different centrality metrics. This systemic impact is computed through an adaptation of the widely used *DebtRank* algorithm developed by Battiston et al. (2012), which we extend to the context of credit hypergraphs. A practical advantage of this method is that it does not require highly detailed information on banks' balance sheets or extensive market valuations, which may be difficult to obtain in emerging market economies or less developed financial systems.

Our main result is that the hypergraph centrality metric proposed in this paper identifies the group of institutions whose distress generates the largest amplified systemic impact, measured as the share of total credit affected in the system. Moreover, the difference between the systemic impact generated by financial institutions identified by this measure and that associated with institutions selected by traditional metrics is statistically significant. This finding has relevant implications for financial supervision and regulation, as the proposed framework may provide complementary tools for analyzing interactions among financial agents, modeling shock amplification, and identifying systemically relevant entities that may not be spotted by conventional indicators. Furthermore, these techniques could be readily applied to other countries and financial systems.

The remainder of the paper is organized as follows. Section 2 describes the empirical credit network under analysis and the database used to construct it. Section 3 presents the main structural properties of the network from a hypergraph perspective. Section 4 introduces several hypergraph centrality measures, compares them with more traditional indicators, proposes an adjustment tailored to the context of bank-firm credit hypergraphs, and reports the results obtained from the alternative institution rankings. In Section 5, we estimate the systemic impact of distress shocks to the most central agents identified by each measure. Finally, Section 6 outlines some concluding remarks.

2. The commercial credit network in Argentina

The main data source used in this paper is the Credit Registry of the Central Bank of Argentina (BCRA), from which monthly credit networks are constructed for the period from August 2023 to December 2025. We focus on loans classified as "commercial", defined as loans granted to firms in connection with their productive activities. Accordingly, personal, mortgage, and consumer loans are excluded from the analysis.

The BCRA suggests a reference threshold for banks to classify loans as "commercial", which is equivalent to twice the maximum annual sales value defined for the "Microenterprise" category in the Commerce sector, as established by the Ministry of Economy. As of December 2025, this maximum sales value was ARS 1,371,080,000[1] (implying a commercial-loan reference threshold of ARS 2,742,160,000), approximately USD 1 million at the exchange rate prevailing at that moment. Although this threshold is not mandatory, and banks may classify smaller exposures within the commercial portfolio, it provides a general reference for the financial system. For this reason, loans are included in the examined network only when the total credit granted to a given company exceeds a minimum threshold equivalent to the December 2025 reference amount. This threshold is adjusted backward for inflation, keeping it constant in real terms throughout the sample period. After applying this criterion and excluding firms with lower outstanding credit, the resulting network captures, on average, 80.3% of total credit to firms. Therefore, it covers a substantial and representative share of the loan universe under examination.

[1] Resolution 54/2025 of the Secretariat for SMEs, Entrepreneurs & Knowledge Economy, under the Ministry of Economy.

On average, 4,132 ± 917 firms[2] and 157 ± 14 financial institutions were active each month during the period analyzed (Figure 2, left), connected through 28,326 ± 5,567 credit relationships per month. The sample includes more than six types of financial institutions (Table 1), but banks account for 98.4% of the credit granted in the commercial segment. Therefore, unless otherwise specified, we will use the terms "financial institutions" and "banks" interchangeably.

Figure 2. **Monthly credit networks: number of nodes and average degree**

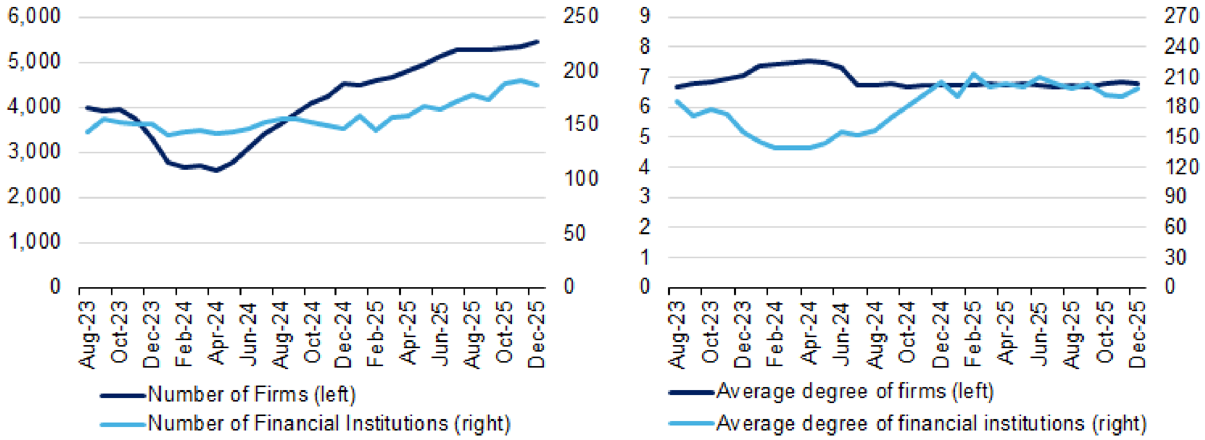

Note: Left: number of lending financial institutions and firms with debt in the financial system (above the minimum threshold). Right: average degree of firms, i.e., the average number of banks from which each firm has borrowed, and of financial institutions, i.e., the average number of firms to which each institution provides credit.

The most basic way to analyze this database using graph theory is through the concept of a bipartite network. This structure consists of two disjoint sets of nodes (financial institutions and firms), where connections can only be established between nodes of different types. Hence, the degree of a node is the number of nodes from the opposite set to which it is connected. In this context, the average degree of a bank corresponds to the average number of firms to which it lends, while the average degree of a firm corresponds to the number of financial institutions from which it receives credit. In the Argentine case, each debtor firm borrowed, on average, from 7 institutions over the period under study, with low variance (Figure 2, right), while each financial institution provided credit to an average of 179 firms. This latter figure exhibits substantial dispersion: banks had an average degree of 368, whereas other types of institutions had significantly fewer connections (Table 1).

Table 1. **Types of financial institutions in the Argentine commercial credit network**

Type of financial institution	Number of institutions	Share of total credit	Average degree (firms per institution)
Banks	69	98.4%	368
NFCCI	7	0.7%	323
ONFCP	60	0.7%	9
Others	20	0.1%	5

Notes: NFCCI: Non-Financial Credit-Card Issuers; ONFCP: Other Non-Financial Credit Providers (mutual associations, credit cooperatives, social clubs, etc.). Others: mutual guarantee institutions, financial trusts, and providers of P2P lending services through platforms.

[2] It should be noted that these figures refer only to firms whose total debt exceeds the reference threshold described above, whereas the complete universe of companies with debt in the financial system exceeds 200,000.

3. Basic topological metrics: bipartite networks, one-mode projections and hypergraphs

As mentioned above, the literature has usually addressed this type of interconnections through the concept of bipartite networks. For example, this perspective has been applied to the analysis of credit networks in Japan (Fujiwara et al., 2009), Italy (De Masi & Gallegati, 2012) and Brazil (Miranda & Tabak, 2013). These networks can be represented by a graph $G(V, U, E)$, composed of two disjoint sets of nodes: V (banks) and U (firms), with $V \cap U = \emptyset$, such that, for every edge $(i, j) \in E$, it must be the case that $i \in V$ and $j \in U$, or vice versa. The matrix representation of these graphs is given by an adjacency matrix A, where, in its basic binary form, each element $a_{ij} = 1$ if there is a loan granted by bank i to firm j, and $a_{ij} = 0$ if there is no credit relationship between the two nodes. It is also possible to work with a weighted matrix W, whose components w_{ij} may represent, for example, the total amount of the loan granted, rather than simply indicating the existence or absence of a relationship in binary form (Figure 3 provides an example of a visualization of this type of network).

Another way to study this object is through a one-mode projection of the adjacency matrix. That is, the original graph can be projected onto the subspace composed of only one type of node (represented by the matrix $P = AA^T$), where two banks are connected if they lend to the same firm. This matrix can be binary, or it can be weighted according to, for example, the number of co-financed firms or the total amount of credit involved in the common exposure. This approach is also widely used in the literature (De Masi et al., 2011; Miranda & Tabak, 2013). The projection onto the set of banks of the bipartite network shown in Figure 3 is displayed in Figure 4.

Figure 3. **Commercial credit relationships as a bipartite network**

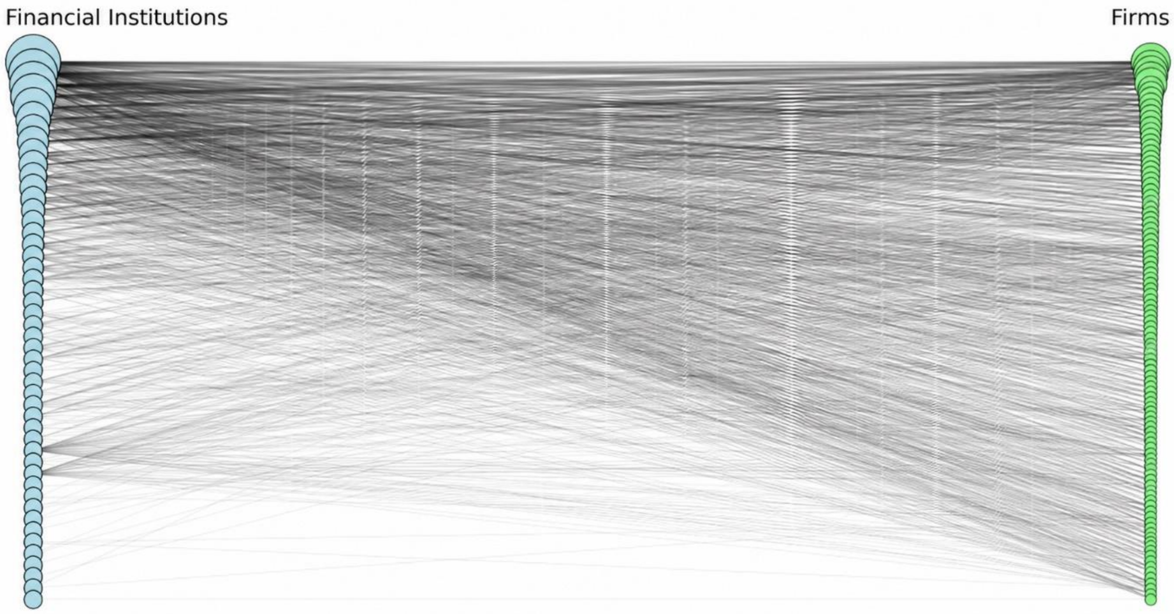

Notes: Bipartite credit network for October 2024. This month was selected because it is the one with the number of nodes closest to the average for the period under study. The size of the circles is associated with the total credit corresponding to each node. The lines represent loans granted by financial institutions (left) to firms (right), and their thickness is associated with the size of the loan. For presentation purposes, this visualization uses a subsample comprising the 50 financial institutions with the largest credit volume and the 100 largest borrowers in their joint portfolio.

Figure 4. **Bank-Bank projection of the commercial credit network**

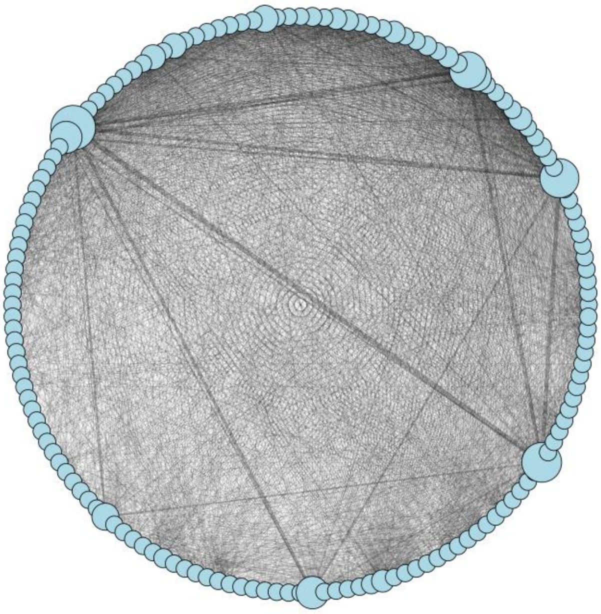

Note: Commercial credit network for October 2024. This month was selected because it is the one with the number of nodes closest to the average for the period under analysis. Node size is associated with the total amount of credit granted by each financial institution. The lines represent common credit exposures among financial institutions to the same firms, and their thickness is correlated with the total amount of joint exposure.

Based on these approaches, it is possible to compute basic topological metrics to examine the structure of interrelations in this network (Figure 5). In the case of the bipartite network, the average density over the period analyzed was 4.5% ± 0.5 p.p., a relatively low value compared with other types of networks but in line with the values observed in empirical financial networks around the world, which usually tend to be sparse (Elosegui et al., 2022; Forte, 2020; Hüser, 2015).

Figure 5. **Basic topological metrics of the bipartite network and its one-mode projection onto banks (monthly networks)**

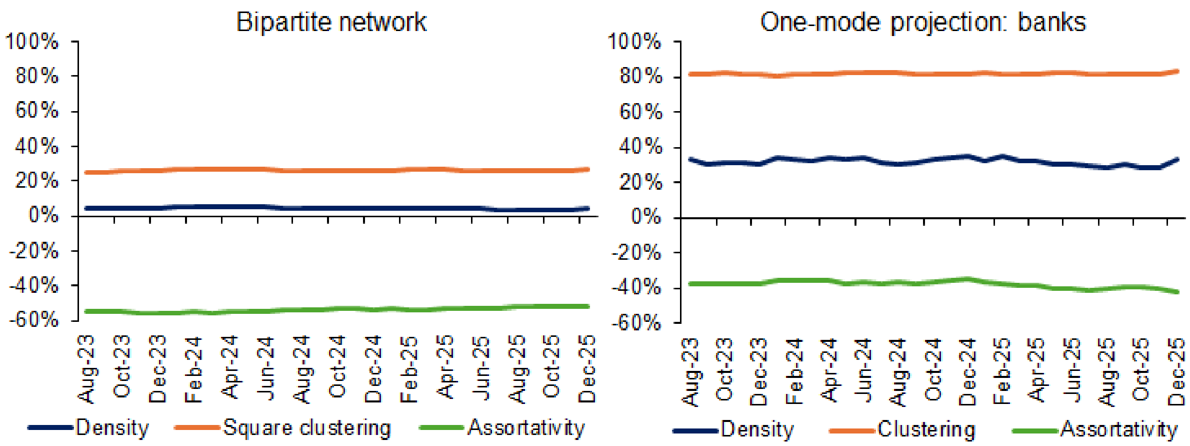

Notes: Left: metrics computed from the unweighted bank-firm bipartite networks. Right: topological metrics of the one-mode projection of the original adjacency matrix onto the set of banks.

The clustering coefficient of these networks[3] averaged 26.4% ± 0.5 p.p., also in line with the values typically observed in financial networks. Finally, the network is clearly disassortative, meaning that

[3] The traditional clustering coefficient captures the share of potential triangles that are actually observed. Because triangles cannot occur in bipartite networks, we instead use the *square clustering* coefficient, which measures the prevalence of

highly connected banks tend to lend comparatively more to less connected firms than less connected banks, and vice versa. Disassortativity is a predominant feature of real-world financial networks. None of these metrics exhibited large changes or significant volatility during the period analyzed.

When the same network is instead examined through its one-mode projection onto banks, attention shifts to the pattern of connections generated by banks' common exposures to the same firms (Figure 5, right). A distinctive feature of this approach is that it mechanically inflates connectivity metrics, since each firm borrowing from multiple banks generates connections among all of them. This is reflected in the average network density, which rises to 32% ± 1.9 p.p., and also in the clustering coefficient (now measured as the ratio of total triangles to possible triangles), which reaches the high value of 82% ± 0.5 p.p. These connectivity levels in financial networks are usually found only in this type of projections, since in other empirical networks (e.g., interbank loans, credit, and payment networks) these metrics tend to be significantly lower. It is also worth noting that the disassortative mixing persists: banks with fewer connections tend to be linked through common exposures (loans to the same firms) to highly connected banks rather than to banks with a similar degree[4].

In this paper, we propose using hypergraphs to provide a more insightful representation of the structure of interconnections in bank-firm credit networks. Hence, this type of networks can be represented as a hypergraph $H(V, E)$, consisting of a set of nodes $V = \{i_1, \dots, i_n\}$, which correspond to lending financial institutions, and a set of links E. The key difference with the traditional approach is that a link is no longer restricted to a pair (i, j), and, instead, each element of E is itself a set that may contain two, three, or more institutions. Thus, relationships are not necessarily bilateral (although bilateral relationships remain possible) but may simultaneously involve multiple institutions. These links are known as *hyperedges*, and their *size* is determined by the number of nodes they contain. Hyperedges may also be weighted through a function $w: E \to \mathbb{R}$, where $w_i(e)$ denotes the weight of node i's participation in hyperedge e. A hypergraph is said to be m-uniform when all its hyperedges have the same size m, although this is rarely the case in real-world applications.

Applying this approach to the credit network, when one or several firms have outstanding debt with a set of m banks, this joint exposure can be represented as a hyperedge. The resulting hypergraph therefore contains only one type of node (financial institutions), while each hyperedge represents a unique set of creditor banks lending to the same firm or firms. Firms borrowing from exactly the same set of banks are thus associated with the same specific hyperedge.

In the Argentine credit network examined here, the average number of hyperedges per month was 3,455 ± 638, with a mean size of 6.9 ± 0.3 banks per hyperedge (weighted by the number of debtor firms). The modal hyperedge size was 5.3 ± 0.5 (Figure 6, left). Thus, the most common sets of banks sharing the same exposure typically range from five to seven institutions, showing a substantial departure from the dyadic representation provided by conventional graphs.

The hypergraphs under analysis are far from uniform, as their hyperedge sizes range from 2 to 36 banks (Figure 6, right). As discussed in the next section, this lack of uniformity poses analytical challenges for the application of some conventional methods.

four-node cycles (that is, configurations in which two banks are both connected to the same two firms), as in Lind et al. (2005) and Luu & Lux (2018).

[4] Disassortative mixing persists even when links are weighted by loan amounts.

Figure 6. **Characteristics of hyperedges in the monthly hypergraphs**

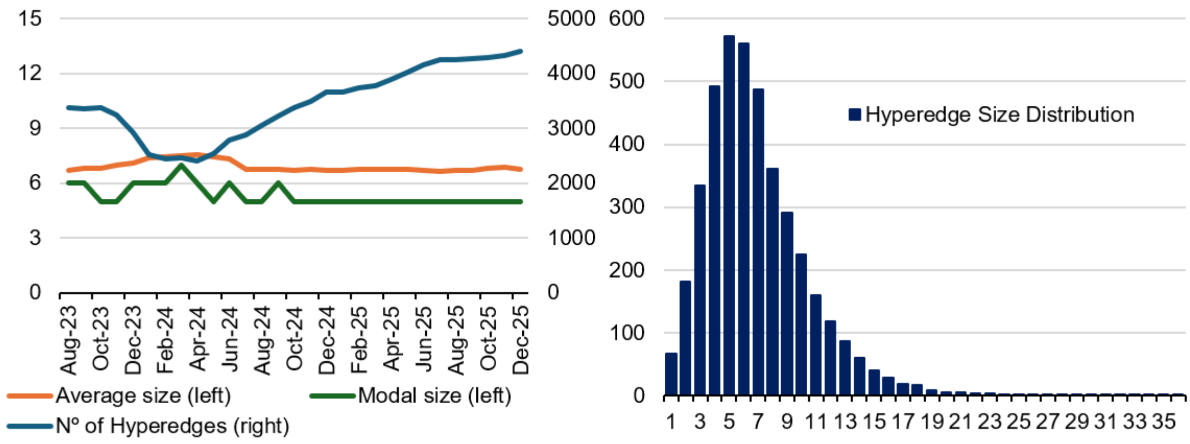

Note: Left: Number of distinct hyperedges in each monthly hypergraph, together with their mean and modal sizes (weighted by the number of debtor firms in each hyperedge). Right: Histogram of the average monthly frequency distribution of hyperedge sizes over the period under analysis.

4. Identification of systemically important financial institutions

Bipartite networks: traditional metrics

Financial supervisors around the world apply methods from the network theory toolkit to identify systemically important financial institutions (BCBS, 2024; FSB-IMF-BIS, 2009). The objective is to subject these institutions to special regulatory frameworks in order to minimize the potential systemic risks arising from their failure (Alaeddini et al., 2023; Martinez-Jaramillo et al., 2019).

The most traditional centrality measures include node *degree* (which, in this context, corresponds to the number of firms to which a bank lends), node *strength* (measured here as the total amount lent by each bank in a given month) and *eigenvector centrality*:

$BIP\_Degree_i = \sum_{\forall j \neq i} a_{ij}$ (I)

$BIP\_Strength_i = \sum_{\forall j \neq i} w_{ij}$ (II)

$ONE\_Eigenvector_i = x_i,$ such that $\lambda \boldsymbol{x} = A\boldsymbol{x}$ (III)

The first two measures are computed directly from the original bipartite network, as is common practice in financial supervision worldwide. Basically, they point to those institutions that: a) reach the highest number of borrowers (degree), or b) lend the highest amount of money in the system (strength).

By contrast, the standard definition of eigenvector centrality requires a square adjacency matrix, since the centrality value of a node i corresponds to the i-th entry of the eigenvector associated with its leading eigenvalue. Hence, this last centrality metric can only be extracted from the one-mode projection of the original bipartite matrix, which yields a square bank-bank matrix. Specifically, the bank-bank projection is constructed from the bipartite network weighted by loan amounts in real terms. Intuitively, this method detects those institutions that are linked to the most connected neighbors in the system, which means that they could be "*too-interconnected-to-fail*", while the strength or degree measures intend to identify the institutions commonly described as "*too-big-to-fail*".

Centrality measures in hypergraphs

Under a hypergraph framework, the analysis no longer relies on adjacency matrices. Instead, the object of study becomes a higher-order tensor, or hypermatrix, with a more complex multidimensional structure. Building on recent advances in the literature that extended the notion of eigenvalues to higher-order tensors and hypermatrices (Qi & Luo, 2017), several measures have been proposed to generalize eigenvector centrality to the context of hypergraphs. One of the most prominent is known as H-eigenvector centrality (Benson, 2019). This measure generalizes the notion of eigenvectors to higher-dimensional settings. In other words, it preserves the same intuition as the original concept, whereby the centrality of a node depends on the centrality of its neighbors, while simultaneously allowing for the nonlinearities that arise in environments characterized by multilateral relationships.

Tensors provide a useful algebraic representation for hypergraphs. Broadly speaking, they generalize matrices to higher-order dimensions. Thus, given an m-uniform hypergraph $H = (V, E)$, where V denotes the set of nodes and E the set of hyperedges, an adjacency tensor (or hypermatrix) T can be defined as follows:

$$T_{i_1,\ldots,i_m} = \begin{cases} 1 & if\ (i_1, \ldots, i_m) \in E \\ 0 & otherwise \end{cases}$$

where $T_{i_1,\ldots,i_m}$ is analogous to the adjacency matrix A for the bilateral case. Relationships can be defined in binary form, as in the equation above, or by incorporating a weight $w(\{i_1, \ldots, i_m\})$, which in our case essentially reflects the amount lent by each of the financial entities $\{i_1, \ldots, i_m\}$ within each hyperedge.

Given this tensor representation, if the hypergraph is strongly connected, there exists a centrality vector **c** that satisfies the following condition:

$$c_i^{m-1} = \frac{1}{\lambda} \sum_{i_2,\ldots,i_m=1}^{n} T_{i i_2 \ldots i_m} c_{i_2} \ldots c_{i_m} \Rightarrow \lambda c^{[m-1]} = T c^{m-1}$$

where $\boldsymbol{c}^{[m-1]}$ denotes the component-wise $(m-1)$-th power of **c**. The centrality vector **c** is then computed iteratively using the power method, in order to obtain the dominant H-eigenvector and, accordingly, the *H-eigenvector centrality* associated with each financial institution.

Other types of eigenvectors have been proposed in the context of hypergraphs (Benson, 2019; Qi & Luo, 2017), but we focus on the H-eigenvector for several reasons: it is less computationally demanding, it admits a unique solution under weaker assumptions than alternative approaches, and it captures the richness of the nonlinear nature of multilateral relationships in hypergraphs without reducing them to a dyadic setting (as some alternative methods do).

A difficulty that arises when applying this centrality computation to financial networks is that it requires the hypergraph to be m-uniform; that is, all hyperedges must contain the same number m of nodes, or equivalently, all hyperedges must have homogeneous size[5]. This is not usually the case in empirical applications, and it is certainly not the case here. Moreover, if each m-uniform sub-hypergraph were analyzed separately, the complexity of the actual hypergraph would be lost, along with substantial interdependencies among hyperedges of different sizes within the network.

[5] This requirement is analogous to the traditional square-matrix condition in standard spectral analysis to compute eigenvalues, extended to the tensor setting through the need for an m-uniform hypergraph.

To overcome this limitation, several methodological strategies have recently been proposed. We briefly discuss below three approaches that have been developed in the literature to address this issue:

1) The first approach proposed to quantify centrality values in non-uniform hypergraphs was the notion of *vectorial centrality score*. Instead of just a single centrality value assigned to each node, a centrality vector is constructed for each node i, $\boldsymbol{v}^i \in \mathbb{R}^{m-1}$, where each component of the vector represents the centrality value of that node in the corresponding m-uniform sub-hypergraph. A drawback of this solution is that, once the hypergraph is decomposed according to the size of its hyperedges, the resulting sub-hypergraphs may fail to be strongly connected. Moreover, this decomposition disregards part of the higher-order interdependence among hyperedges of different sizes that characterizes the original network structure. Hence, Kovalenko et al. (2022), in order to address that limitation, suggested using the incidence matrix of the hypergraph (whose rows correspond to nodes and the columns to hyperedges), and projecting it onto the set of hyperedges. This yields a square matrix, namely the *line graph* derived from the hypergraph. On this object, the centrality of the edges can be computed using traditional procedures, such as the classical eigenvector centrality. Once the centrality of each hyperedge -$c(h)$- has been computed, the authors suggest defining node centrality as the sum of the centralities of the hyperedges in which the node participates. More specifically, they propose constructing, for each node i, a normalized vector $\boldsymbol{c_i} \in \mathbb{R}^{m-1}$, where each of its k components is given by:

$$c_{ik} = \frac{1}{k} \sum_{\substack{i \in h \in E \\ |h| = k}} c(h)$$

where $c(h)$ denotes the centrality value of hyperedge h, and $|h|$ refers to the size of that hyperedge. The authors show that this vector is normalized.

2) A second proposal was put forward by Tudisco and Higham (2021), who introduce a family of spectral centrality measures for non-uniform hypergraphs, which allows a simultaneous computation of the relative importance of both the nodes and hyperedges. The central idea is to extend the logic of eigenvector centrality in traditional graphs to settings in which interactions are not necessarily bilateral, but rather of higher order. Under this notion, in a simple graph a node is central if it is connected to other central nodes. In a hypergraph, by contrast, a node may participate in hyperedges that group several nodes at once. The authors therefore propose a mutually reinforcing relationship: a node is important if it participates in important hyperedges, and a hyperedge is important if it contains important nodes. This formulation makes it possible to capture the higher-order interaction structure without reducing the hypergraph to a clique projection or to a network of pairwise relations.
Starting from the incidence matrix of the hypergraph, Tudisco and Higham formulate a nonlinear eigenvalue problem that generalizes both traditional eigenvector centrality and some tensor-based measures for uniform hypergraphs. The flexibility of the approach arises from the choice of certain nonlinear functions that determine how node centralities are aggregated within each hyperedge and how hyperedge centralities are aggregated at each node. They study three main specifications: a linear version, similar to eigenvector centrality applied to the bank projection and to the line graph; a "log-exp" version, which generalizes tensor-based Z-eigenvector centrality; and a "max" version, which assigns high centrality to nodes that participate in at least one highly important hyperedge. The result is a family of three measures that can be adapted to different assumptions about how centrality is transmitted within group interactions (see Appendix A for details on the mathematical formulation).

3) Finally, the most recent proposal (and the one discussed in greater depth in this paper) is that of Contreras-Aso et al. (2024). They propose a "uniformization" method for making hyperedge sizes equal in hypergraphs that are originally non-uniform. Once the baseline hypergraphs have been "made" uniform, H-eigenvector centrality measures can be computed in the same way as in the benchmark case described above. The main idea they propose is to "expand" the size of smaller hyperedges by adding "artificial auxiliary nodes" weighted in such a way that their impact on the centrality metrics is neutral. They refer to this procedure as the "*uplift*" of smaller hyperedges. In addition, they also propose "shrinking" larger hyperedges to a smaller size, such as p. To do so, they suggest decomposing ("*projecting*") each hyperedge of size $k > p$ into all possible $C(k,p) = \binom{k}{p}$ combinations of smaller hyperedges of size p (see Appendix B for further details on the mathematical formulation of this proposal).

To compute this third type of centrality using the method proposed by Contreras-Aso et al., it is necessary to define the size to which all hyperedges in the hypergraphs under analysis should be "uniformized". We propose two alternative strategies: (1) setting all hyperedges to the modal size by uplifting the smaller hyperedges and projecting the larger ones; or (2) increasing the size of all hyperedges to the maximum observed size, or at least to a size that covers a significant share of the amount lent in the system (here, we uplift all hyperedges up to size 19, a level chosen because hyperedges of up to this size account for at least 80% of the total amount lent in the networks in every month under analysis, while hyperedges larger than this value are discarded[6]).

In this paper we propose a complementary refinement of the algorithms developed by Contreras-Aso et al. (2024) for the computation of centrality in financial hypergraphs. The original formulation calculates the centrality of each node i as a function of the centrality of its neighboring nodes within the hyperedges in which it participates. In the context of credit networks, the standard weighted version of this measure would assign to each interaction the total weight of the shared hyperedge. Here, we keep that idea but weight the centrality of those neighboring nodes by the amount that the node i lends in each hyperedge in which it participates. This adjustment avoids the potential bias of identifying as relevant those nodes that, for example, participate in large transactions alongside highly central banks while contributing only small amounts, or small shares of their own portfolios, which may not adequately reflect their core activity. If neighbors' centrality is not weighted by the node's own contribution, the measure may overstate the relevance of small or secondary banks whose relevance derives mainly from participating with minor amounts in transactions largely driven by more central banks.

Mathematically, the complementary refinement we propose for computing this weighted version of the H-eigenvector centrality can be formulated as follows:

- The central idea behind the standard H-eigenvector centrality is that the centrality c_i of node i depends on the centrality of the neighboring nodes with which it shares hyperedges. Since nodes have more than one neighbor within each hyperedge (more precisely, $m-1$ neighbors in uniform hypergraphs), this formulation quantifies the joint centrality of the neighboring nodes, c_j, multiplicatively:

[6] Expanding all hyperedges to the maximum observed size (36) would exponentially increase the number of artificial nodes required while adding little information, as only a relatively small share of total loans is concentrated in larger hyperedges.

Standard unweighted H_eigenvector centrality: $\lambda c_i^{m-1} = \sum_{i \in e \in E} \prod_{\substack{j \in e \\ j \neq i}} c_j$

- The weighted version of this centrality measure, where weights are given by the amount of credit involved in each hyperedge, can be written as:

  Standard weighted H_eigenvector centrality: $\lambda c_i^{m-1} = \sum_{i \in e \in E} w_e \prod_{\substack{j \in e \\ j \neq i}} c_j$

  where w_e denotes the total amount of credit involved in each hyperedge.

- However, in the context of financial networks, we argue that identifying central agents in credit networks requires more than examining the centrality of the neighbors with which a bank shares credit transactions and the total amount associated with the hyperedge. It is also relevant to account for how much *each* entity contributes to these joint exposures. Otherwise, small or relatively marginal entities may be classified as important merely because they participate in large hyperedges with highly connected banks, even if they consistently do so with small amounts that are not systemically relevant. For this reason, we propose weighting separately the contribution of each entity to the corresponding hyperedge, thereby disaggregating the weight assigned to each node involved in the shared exposure. Mathematically, our proposal is the following:

  H_eigenvector centrality weighted by individual contribution to each hyperedge:

$$\lambda c_i^{m-1} = \sum_{i \in e \in E} h_{ie} \prod_{\substack{j \in e \\ j \neq i}} h_{je} c_j$$

  Where h_{ie} is the amount lent by node i in hyperedge e. In summary, the proposed centrality measure *multiplicatively* incorporates *both* the amount lent by each entity in each hyperedge and the centrality of the nodes sharing those hyperedges. This formulation therefore nonlinearly combines the relevance of each node's neighbors, the importance of the hyperedges in which it participates, and the individual contribution of node i to each corresponding hyperedge.

To summarize, Table 2 reports all the centrality metrics that will be applied to the credit network under analysis, with the aim of quantifying, through alternative methods, the relative relevance of the central agents in the system.

After computing the centrality rankings of financial institutions for all months in the sample, we compare the results using Kendall rank correlations and the top-20 overlap of entities identified by each of the metrics described in Table 2. In general, all rankings obtained from the different centrality measures display positive and relatively high Kendall correlations (Figure 7 shows the average correlations throughout the period analyzed). The lowest correlation among all possible pairs is 0.59, while the overall average pairwise rank correlation is 0.73. Nonetheless, there are some groups of metrics that are comparatively more similar to one another. The results derived from the hypergraph-based indicators proposed by Tudisco and Higham (*HYP_TH_lin*, *HYP_TH_logexp*, and *HYP_TH_max*) yield the most similar results to those obtained from traditional metrics based on bipartite graphs (such as degree and strength), or on the bank-bank projection (*ONE_eigenvector*). In other words, these metrics tend to provide less additional information relative to the more conventional approaches. The vectorial centrality measure (*HYP_VC*) exhibits somewhat lower correlation with traditional metrics. By contrast, the metrics that display the lowest correlations with traditional measures are those obtained from the computation of H-eigenvectors (*HYP_HE_uplift* and *HYP_HE_upproj*). This would suggest, *a priori*, that the latter may be the measures with the greatest potential to provide new information relative to the approaches based on graphs with dyadic connections.

Table 2. **Summary of the centrality measures computed in this paper**

	Graph	Centrality	Abbreviation	Description
(I)	Bipartite	Degree	*BIP_degree*	Number of borrowers
(II)	Bipartite	Strength	*BIP_strength*	Total amount lent
(III)	One-mode projection (banks)	Eigenvector	*ONE_eigenvector*	The centrality of a node depends on the centrality of its neighbors
(IV)	Non-uniform hypergraph	Vectorial Centrality	*HYP_VC*	Sum of the centrality of the hyperedges in which each node participates
(V)	Non-uniform hypergraph	Tudisco & Higham (2021) - linear model	*HYP_TH_lin*	A node is central if it participates in important hyperedges
(VI)	Non-uniform hypergraph	Tudisco & Higham (2021) - logexp model	*HYP_TH_logexp*	Node centrality depends on the product of the centralities of its hyperedge neighbors
(VII)	Non-uniform hypergraph	Tudisco & Higham (2021) - max model	*HYP_TH_max*	A node is central if it belongs to at least one highly important hyperedge
(VIII)	Uniformized hypergraph	H-eigenvector: uplift to maximum size	*HYP_HE_ uplift_trad*	Generalization of ONE_eigenvector to uniform hypergraphs
(IX)	Uniformized hypergraph	Same as (VIII), weighted by individual amount lent (multiplicatively)	*HYP_HE_ uplift_adj*	Our proposed adjustment: nonlinearly weights neighbors' centrality and the amount lent in each hyperedge
(X)	Uniformized hypergraph	H-eigenvector: uplift & projection to modal size	*HYP_HE_ upproj_trad*	Generalization of ONE_eigenvector to uniform hypergraphs
(XI)	Uniformized hypergraph	Same as (X), weighted by individual amount lent (multiplicatively)	*HYP_HE_ upproj_adj*	Our proposed adjustment: nonlinearly weights neighbors' centrality and the amount lent in each hyperedge

Figure 7. **Kendall correlations between bank rankings across centrality metrics**

	BIP_ degree	BIP_ strength	ONE_ eigen-vector	HYP_ VC	HYP_TH_ lin	HYP_TH_ logexp	HYP_TH_ max	HYP_HE_ uplift_ trad	HYP_HE_ upproj_ trad	HYP_HE_ uplift_ adj	HYP_HE_ upproj_ adj
BIP_degree	1.00	0.74	0.72	0.79	0.72	0.74	0.74	0.70	0.75	0.68	0.69
BIP_strength	0.74	1.00	0.83	0.69	0.83	0.99	0.94	0.63	0.66	0.66	0.65
ONE_eigenvector	0.72	0.83	1.00	0.78	1.00	0.82	0.87	0.59	0.66	0.67	0.72
HYP_VC	0.79	0.69	0.78	1.00	0.78	0.69	0.71	0.64	0.74	0.72	0.75
HYP_TH_lin	0.72	0.83	1.00	0.78	1.00	0.82	0.87	0.59	0.66	0.67	0.72
HYP_TH_logexp	0.74	0.99	0.82	0.69	0.82	1.00	0.94	0.64	0.66	0.66	0.65
HYP_TH_max	0.74	0.94	0.87	0.71	0.87	0.94	1.00	0.62	0.67	0.66	0.68
HYP_HE_uplift_trad	0.70	0.63	0.59	0.64	0.59	0.64	0.62	1.00	0.73	0.75	0.61
HYP_HE_upproj_trad	0.75	0.66	0.66	0.74	0.66	0.66	0.67	0.73	1.00	0.70	0.79
HYP_HE_uplift_adj	0.68	0.66	0.67	0.72	0.67	0.66	0.66	0.75	0.70	1.00	0.72
HYP_HE_upproj_adj	0.69	0.65	0.72	0.75	0.72	0.65	0.68	0.61	0.79	0.72	1.00

Note: see Table 2 for a description of the abbreviations corresponding to each centrality measure.

Analogous conclusions can be drawn from the computation of the top-20 overlap among the financial institutions selected by each metric (Figure 8). On average, all pairs of indicators coincide in 82% of the entities included among the top 20 most central institutions, while the lowest observed level of overlap is 69%, precisely in the case of H-eigenvector centralities.

Figure 8. **Top-20 overlap among financial institutions identified by each centrality measure**

	BIP_degree	BIP_strength	ONE_eigen-vector	HYP_VC	HYP_TH_lin	HYP_TH_logexp	HYP_TH_max	HYP_HE uplift_trad	HYP_HE uproj_trad	HYP_HE uplift_adj	HYP_HE uproj_adj
BIP_degree	1.00	0.86	0.79	0.94	0.79	0.86	0.86	0.81	0.85	0.76	0.76
BIP_strength	0.86	1.00	0.90	0.86	0.90	0.97	0.98	0.76	0.80	0.77	0.79
ONE_eigenvector	0.79	0.90	1.00	0.82	1.00	0.88	0.91	0.69	0.73	0.78	0.79
HYP_VC	0.94	0.86	0.82	1.00	0.82	0.87	0.86	0.84	0.88	0.80	0.81
HYP_TH_lin	0.79	0.90	1.00	0.82	1.00	0.88	0.91	0.69	0.73	0.78	0.79
HYP_TH_logexp	0.86	0.97	0.88	0.87	0.88	1.00	0.96	0.77	0.80	0.77	0.79
HYP_TH_max	0.86	0.98	0.91	0.86	0.91	0.96	1.00	0.76	0.80	0.77	0.79
HYP_HE_uplift_trad	0.81	0.76	0.69	0.84	0.69	0.77	0.76	1.00	0.96	0.69	0.71
HYP_HE_upproj_trad	0.85	0.80	0.73	0.88	0.73	0.80	0.80	0.96	1.00	0.72	0.74
HYP_HE_uplift_adj	0.76	0.77	0.78	0.80	0.78	0.77	0.77	0.69	0.72	1.00	0.84
HYP_HE_upproj_adj	0.76	0.79	0.79	0.81	0.79	0.79	0.79	0.71	0.74	0.84	1.00

Note: see Table 2 for a description of the abbreviations corresponding to each centrality measure.

5. Systemic impact

In this section, we assess the implications of identifying relevant agents in the financial network according to each of the different centrality measures described above. To this end, we compute the impact on the system resulting from a distress shock to the top-ranked institutions under each of the eleven metrics considered here (Table 2).

Several measures of systemic impact have been developed (Acharya et al., 2017; Adrian & Brunnermeier, 2016; Li & Zhang, 2024; Liu et al., 2024), among which the *DebtRank* algorithm, introduced by Battiston et al. (2012), has become one of the most widely used approaches (Sulas et al., 2025). It is a recursive method that quantifies systemic risk in terms of the potential propagation of financial distress across an economic network. An additional reason for selecting this approach is that it does not require extremely detailed information on banks' balance sheets or market-based asset valuations, which may be difficult to obtain or even unavailable in emerging market economies with less developed financial markets. Previous studies have adapted the *DebtRank* algorithm to credit relationships represented as bipartite networks, for instance in the cases of Brazil (Silva et al., 2018) and Japan (Aoyama et al., 2013). We build on elements of those applications to adapt the algorithm to our bank-firm credit setting, while further extending it to the hypergraph framework.

The exercise proposed here consists of the following procedure. For each month, we take the set of top-k institutions ranked according to a given centrality measure and simulate an initial shock to the credit portfolio of each of these k institutions. Let $H \in \mathbb{R}_+^{N \times E}$ be the weighted incidence matrix of the hypergraph, where N is the number of financial institutions, E is the number of hyperedges, and H_{ie} represents the amount lent by the bank i in hyperedge e. The total portfolio of each financial institution is defined as:

$$L_i = \sum_{e=1}^{E} H_{ie}$$

while the total amount associated with each hyperedge is:

$$B_e = \sum_{i=1}^{N} H_{ie}$$

Given the initial set of affected banks S, corresponding to the top-k institutions according to the centrality measure under analysis, the initially affected amount of credit in the system is defined as:

$$D_i(0) = \begin{cases} L_i & \text{if } i \in S \\ 0 & \text{if } i \notin S \end{cases}$$

The relative distress level of each institution is then defined:

$$h_i(t) = \frac{D_i(t)}{L_i}$$

bounded in the interval $[0,1]$. Initially shocked institutions have $h_i(0) = 1$. Propagation takes place iteratively through a "bank-hyperedge-bank" dynamic. Importantly, at each iteration only the new incremental shock generated between $(t-1)$ and t is considered:

$$\Delta h_i(t) = \max\{h_i(t) - h_i(t-1), 0\}$$

This new incremental distress is transmitted from financial institutions to hyperedges according to the relative participation of the affected institutions in each hyperedge:

$$\Delta g_e(t) = \frac{\sum_{i=1}^{N} H_{ie}\, \Delta h_i(t)}{B_e}$$

The term $\Delta g_e(t)$ therefore measures the new fraction of the hyperedge e that becomes affected at iteration t. This impact on hyperedges is then transmitted back to financial institutions according to their exposure to each hyperedge:

$$\Delta D_i(t+1) = (1 - h_i(t)) \sum_{e=1}^{E} H_{ie}\, \Delta g_e(t)$$

The factor $(1 - h_i(t))$ prevents an institution from receiving a shock larger than its total portfolio, thereby imposing the upper bound $D_i(t) \leq L_i$. The cumulative affected amount is calculated as follows:

$$D_i(t+1) = \min\{L_i, D_i(t) + \Delta D_i(t+1)\}$$

It is then normalized as a share of each institution's initial total portfolio:

$$h_i(t+1) = \frac{D_i(t+1)}{L_i}.$$

The process continues iteratively until the new aggregate distress in the system converges to a value close to zero. Finally, the total systemic impact derived from shocking a set of k banks is defined as:

$$I^{\text{total}} = I^{\text{direct}} + I^{\text{amplified}}$$

where $I^{\text{direct}} = \sum_{i \in S} L_i$ is the total amount of credit initially affected, and $I^{\text{total}} = \sum_{i=1}^{N} D_i\,(T)$, with T denoting the last iteration. Thus, I^{total} represents the total systemic impact, in terms of the amount of credit affected, after the iterative propagation dynamics of the initial shock have concluded. The indirect, or amplified, impact is therefore obtained as the difference between these two values. These impacts are reported below as a percentage of the total amount of credit in the network.

In summary, the algorithm measures how much credit in the system becomes affected when the most important banks according to each centrality metric are initially shocked. The hypergraph structure allows propagation to occur not only through bilateral links, but also through co-financing configurations that simultaneously involve multiple financial institutions.

To compare the systemic risk arising from the top-ranked institutions identified by each metric, we focus on the indirect, or amplified, effect rather than on the initial shock, in order to specifically quantify the incremental contagion generated by each set of institutions. This approach is consistent with Aoyama et al. (2013), Bardoscia et al. (2015) and Silva et al. (2018), and is intended to avoid conclusions driven by the initial size of the institutions rather than by their potential to propagate financial distress throughout the network.

Figure 9. **Amplified systemic impact of shocking the top-ranked financial institutions identified by each centrality metric** (% of total credit in the system)

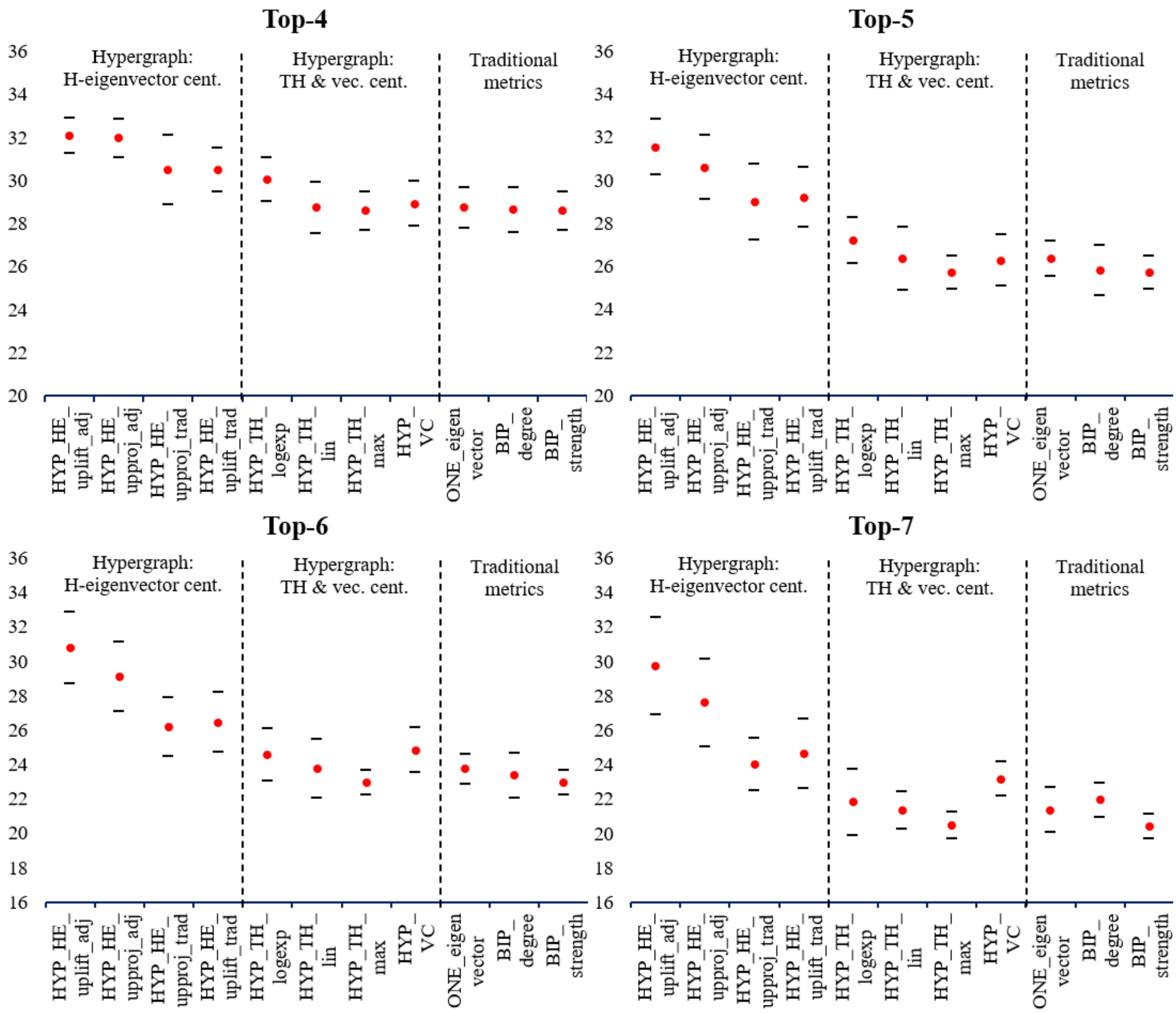

Notes: Each panel shows the average amplified impact across all months under analysis obtained by shocking the top-k financial institutions identified by each centrality measure (for k = 4, 5, 6, and 7). The black lines indicate a range of ±1 standard deviation. See Table 2 for a summary of the centrality metrics and their abbreviations.

The comparison of the amplified systemic impact generated by shocks to the top-ranked institutions selected according to each centrality metric (Figure 9) yields a clear result: H-eigenvector centrality metrics computed on uniformized hypergraphs identify the set of institutions with the greatest shock-amplification effect. The metrics proposed by Tudisco and Higham and the vectorial centrality measure display more variable results, but they do not consistently outperform traditional metrics such as degree, strength, or eigenvector centrality derived from bipartite networks or their one-mode projections.

These results remain robust when considering different sizes of the top-k sets, as shown in Figure 9. From top-1 to top-3, the rankings do not change substantially across centrality metrics. Meaningful differences in terms of systemic impact begin to emerge from top-4 rankings onward[7].

In particular, the largest amplified impact is generated in every month of the period under analysis by the central agents identified according to the metric proposed in this paper: H-eigenvector centrality computed on hypergraphs uniformized through the methods of Contreras-Aso et al., with centrality scores weighted by the amounts contributed by each bank to each hyperedge (*HYP_HE_uplift_adj* and *HYP_HE_upproj_adj*). This metric consistently captures a higher level of systemic-amplification risk than all the others.

Table 3. **Differential impact of shocks to top-ranked financial institutions: traditional centrality metrics versus H-eigenvector centrality measures** (percentage points; 95% confidence intervals in brackets; differences computed as row minus column)

	Shocked top-ranked institutions	**BIP_degree**	**BIP_strength**	**ONE_eigenvector**
HYP_HE_uplift_adj	**Top-4**	3.49 [2.64, 4.37]	3.50 [2.73, 4.38]	3.35 [2.44, 4.25]
	Top-5	5.73 [4.76, 6.79]	5.84 [4.85, 6.94]	5.18 [3.98, 6.30]
	Top-6	7.40 [6.32, 8.68]	7.83 [6.66, 9.13]	7.00 [5.41, 8.55]
	Top-7	7.80 [6.27, 9.59]	9.33 [7.86, 10.91]	8.38 [6.68, 10.07]
HYP_HE_upproj_adj	**Top-4**	3.33 [2.61, 4.06]	3.38 [2.72, 4.12]	3.23 [2.47, 3.99]
	Top-5	4.79 [4.05, 5.61]	4.90 [4.18, 5.69]	4.23 [3.23, 5.26]
	Top-6	5.72 [4.47, 7.09]	6.15 [5.19, 7.41]	5.32 [4.19, 6.65]
	Top-7	5.66 [3.99, 7.54]	7.19 [5.81, 8.85]	6.24 [4.87, 7.73]
HYP_HE_uplift_trad	**Top-4**	1.85 [1.18, 2.56]	1.91 [1.25, 2.63]	1.75 [1.11, 2.48]
	Top-5	3.38 [2.75, 3.97]	3.49 [2.79, 4.09]	2.83 [1.93, 3.67]
	Top-6	3.10 [2.66, 3.81]	3.52 [2.96, 4.21]	2.70 [1.86, 3.47]
	Top-7	2.71 [1.99, 3.78]	4.24 [3.67, 4.96]	3.29 [2.52, 4.13]
HYP_HE_upproj_trad	**Top-4**	1.86 [1.23, 2.58]	1.91 [1.30, 2.66]	1.76 [1.09, 2.50]
	Top-5	3.17 [2.48, 3.81]	3.28 [2.54, 3.97]	2.61 [1.70, 3.58]
	Top-6	2.83 [2.15, 3.56]	3.26 [2.47, 4.06]	2.43 [1.37, 3.35]
	Top-7	2.07 [1.37, 2.99]	3.60 [3.03, 4.27]	2.65 [1.99, 3.39]

Notes: Each value reflects the average difference (in p.p.) between the amplified systemic impact of shocking the top-k financial institutions identified by the centrality measure shown in the row and the corresponding impact obtained for the top-k financial institutions identified by the centrality measure shown in the column. A 95% confidence interval is reported in brackets, computed through block-bootstrapping, with a block size of 3 to account for potential autocorrelation. The intervals do not change significantly when alternative block sizes are used.

[7] For set sizes $k \geq 8$, the initially shocked institutions account for more than 70% of total credit, causing distress to spread rapidly throughout almost the entire network regardless of the centrality measure used.

With respect to the hypergraph uniformization criterion, we cannot conclude that any single approach consistently captures the largest systemic impact. Although, on average, the largest effect is obtained through uplifting, in some months the combination of uplifting smaller hyperedges and projecting larger ones to the modal size captures a higher systemic impact. However, one or both of these two metrics consistently capture the greatest potential for shock amplification relative to the other measures.

Table 3 shows the average difference in the amplified systemic impact caused by the top-k institutions identified by H-eigenvector centrality measures versus the traditional ones (degree, strength and eigenvector centrality), together with the corresponding 95% confidence intervals computed through block-bootstrapping. In all cases, the differences in amplified systemic impact are statistically significant, ranging from nearly 2 to 9 p.p. of total credit in the system, with H-eigenvector centrality measures consistently identifying the sets of institutions associated with higher propagation risk.

An additional robustness exercise is presented in Appendix C, where the same systemic impact is computed, but using the original bipartite network (rather than the hypergraph representation) and applying the version of the DebtRank algorithm appropriate to that setting. The results remain virtually identical, both in terms of the estimated systemic impact and statistical significance.

6. Concluding remarks

This paper proposes the use of hypergraphs to provide a more comprehensive analysis of the structure of credit relationships between financial institutions and firms. In this context, the joint exposures of multiple banks to a firm can be more naturally understood as an underlying multilateral relationship among all institutions lending to that borrower. Representing these relationships as collections of pairwise interactions may hide relevant information arising from potential amplification effects that simultaneously involve multiple agents.

Bipartite networks preserve the identity of each borrower and its lenders, but the centrality measures most commonly applied to them rely on dyadic connections. One-mode projections further compress each borrower-specific lending group into a collection of bank-bank ties. These approaches therefore do not directly evaluate the full set of lenders associated with a borrower as a higher-order interaction. The hypergraph representation used here explicitly preserves this group structure and makes it possible to apply nonlinear centrality operators to sets of creditor institutions linked by common borrowers.

One of the main contributions of the proposed framework lies in the identification of systemically relevant institutions. We compare the most relevant institutions identified by a range of centrality measures, from traditional indicators to more recently developed hypergraph-based metrics. We also propose an adjustment to the weighted H-eigenvector centrality after uniformizing hyperedge sizes following Contreras-Aso et al. (2024). Our adjustment assigns institution-specific weights based on the amount lent by each creditor within each hyperedge. The resulting measure jointly captures two key dimensions of an institution's relevance: on the one hand, how much each institution lends in the network (as a proxy for its size), and, simultaneously, its position within a structure of multilateral relationships characterized by nonlinear interactions. In other words, it multiplicatively combines an institution's relevance in terms of its lending volume with both its own connectivity and the connectivity of its neighbors, within a framework of higher-order relationships.

Based on the centrality rankings of nodes obtained from these measures, we quantify the systemic impact associated with the top-ranked institutions according to each metric. When measuring systemic impact, it is important to note that we focus on the *incremental* distress amplified through the system rather than on the initial shock itself. This distinction allows us to isolate the potential for distress propagation from the initial size of the portfolios of the shocked institutions.

The results show that the greatest amplification effects are generated by the institutions identified by the measure proposed here: the adjusted H-eigenvector centrality. This measure consistently detects sets of institutions whose joint shock-amplification effect is statistically higher than that associated with institutions selected by traditional metrics (measured as a share of total commercial credit in the system). These findings remain robust across different sizes of the set of top-ranked institutions and when distress propagation is modeled using either the hypergraph representation or the original bipartite network.

Our findings have relevant implications for banking supervision and regulation. The proposed framework provides a novel criterion for detecting institutions with greater potential for distress amplification than those selected by alternative centrality measures. These techniques could therefore complement existing supervisory criteria for assessing systemic importance and can be readily applied across different countries and financial systems.

Looking ahead, the research agenda remains fertile, as the application of hypergraphs to financial networks is still at a very early stage. First, our study focused on a specific channel of financial interconnectedness (commercial credit relationships between financial institutions and firms) and on the potential propagation of distress through this network structure. Extending the framework to incorporate alternative mechanisms of distress transmission could provide useful complementary assessments of systemic risk. Other potentially valuable avenues for future research include: a) incorporating the temporal dimension of hypergraphs to study dynamic patterns; b) integrating additional layers of the financial system, such as overlapping portfolios or interbank transactions; and c) developing probabilistic models of agent behavior in environments characterized by multilateral interactions. Statistical methods based on hypergraphs are also developing rapidly, and new tools within this framework are likely to continue emerging, allowing for a deeper analysis of multilateral interactions among financial institutions.

7. Appendices

Appendix A. Node and edge nonlinear eigenvector centrality for hypergraphs (Tudisco & Higham, 2021)

Let $H = (V, E)$ be a hypergraph with n nodes and m hyperedges. The structure of the hypergraph can be represented by an incidence matrix $B \in \mathbb{R}^{n\times m}$, whose elements are defined as

$$B_{i,e} = \begin{cases} 1 & \text{if } i \in e, \\ 0 & \text{otherwise} \end{cases}$$

The framework proposed by Tudisco and Higham allows weights to be incorporated for both nodes and hyperedges. To this end, two diagonal matrices are introduced: N, associated with node weights, and W, associated with hyperedge weights. Node centrality is represented by a positive vector $x \in \mathbb{R}^n_+$, while hyperedge centrality is represented by a positive vector $y \in \mathbb{R}^m_+$. The general formulation consists of solving the following nonlinear system:

$$\lambda x = g\big(BWf(y)\big),$$

$$\mu y = \psi\left(B^T N \varphi(x)\right),$$

where f, g, φ and ψ are functions acting component-wise, and $\lambda, \mu > 0$ are normalization scalars. The first equation indicates that the centrality of each node depends on the centrality of the hyperedges in which it participates. The second equation indicates that the centrality of each hyperedge depends on the centrality of the nodes it contains. Therefore, the measure is defined as a nonlinear eigenvector problem, in which node and hyperedge centralities are jointly determined.

A1. Linear model. The first case considered by the authors is obtained by setting

$$f = g = \varphi = \psi = \mathrm{id},$$

where id denotes the identity function. In this case, the previous system reduces to a linear formulation:

$$\lambda x = BWy,$$
$$\mu y = B^T N x.$$

This specification is analogous to a HITS-type centrality. Nodes define their centrality from the hyperedges to which they belong, while hyperedge centrality is determined by the nodes they contain. In other words, a node is central if it participates in central hyperedges, and a hyperedge is central if it is composed of central nodes. In the case of an ordinary graph, this formulation is related to the computation of eigenvector centrality in the original graph and in the line graph. In hypergraphs, it can be interpreted as a spectral centrality associated with projections of the incidence matrix onto nodes and/or hyperedges.

A2. Log-Exp Model. The second model is obtained from the following choice of functions:

$$f(x) = x$$
$$g(x) = \sqrt{x}$$
$$\varphi(x) = \ln(x)$$
$$\psi(x) = \exp(x)$$

This specification introduces a multiplicative form of aggregation. In particular, the centrality of a hyperedge depends on the product of the centralities of the nodes that compose it. For a hyperedge e, this yields an expression of the form

$$\mu y_e = \exp\left(\sum_{j \in e} \nu\,(j) \ln(x_j)\right) = \prod_{j \in e} x_j^{\nu(j)}$$

where $\nu(j)$ represents the weight of node j. When node weights are binary, this formulation can be interpreted as a non-uniform generalization of tensor-based Z-eigenvector centralities.

The intuition behind the model is that hyperedges are more central when they are composed of central nodes. However, by relying on multiplicative aggregation, the presence of a node with low centrality significantly reduces the centrality of the entire hyperedge. Therefore, this specification penalizes hyperedges that contain less relevant nodes.

A3. "Max" Model. The third model is based on an approximation of the maximum function through a high-order norm. In this case, the authors set

$$f = g = \mathrm{id}$$
$$\varphi(x) = x^{\alpha}$$

$$\psi(x) = x^{1/\alpha}$$

with $\alpha = 10$. The idea behind this specification is that, for high values of α,

$$\left(v_1^{\alpha} + \cdots + v_m^{\alpha}\right)^{1/\alpha} \approx \max\{v_1, \dots, v_m\}$$

In this way, the centrality of a node can be approximated by

$$x_i \approx \max\{y_e : i \in e\}$$

Intuitively, this model assigns high centrality to a node if it participates in at least one highly important hyperedge. Unlike the linear model, it does not add up the contribution of all hyperedges in which the node participates; and unlike the log-exp model, it does not require all those hyperedges to be composed of central nodes. Instead, it approximates a logic of "maximum exposure": the importance of the node is determined primarily by its participation in the most relevant hyperedge.

A4. Non-linear Power Method. From a computational perspective, Tudisco and Higham show that, under certain homogeneity and monotonicity conditions on the functions involved, the problem admits a unique positive solution, up to scaling. This solution can be approximated through a nonlinear power method.

The algorithm starts from positive initial vectors for x and y, and then proceeds by iteratively alternating between node and hyperedge centrality updates. At each iteration, x is updated on the basis of the current values of y, after which y is updated using the newly computed values of x. After each step, both vectors are normalized to control for scale. The procedure is repeated until the change between successive iterations becomes sufficiently small.

In applied terms, this approach makes it possible to obtain simultaneously a ranking of nodes and a ranking of hyperedges in large, weighted, non-uniform hypergraphs. This feature is especially useful when the aim is to evaluate the relative importance of nodes not only according to the number of hyperedges in which they participate, but also according to the endogenous importance of those hyperedges and of the other nodes that compose them.

Appendix B. Uplift and Projection procedures for the uniformization of non-uniform hypergraphs (Contreras-Aso et al., 2024)

In non-uniform hypergraphs, hyperedges may have different sizes. This poses an obstacle to the direct application of tensor-based spectral measures, such as H-eigenvector centrality, since these measures are naturally formulated for m-uniform hypergraphs (that is, hypergraphs in which all hyperedges have the same size). Contreras-Aso et al. propose addressing this problem through a hypergraph uniformization procedure that combines two operations: the uplift of lower-order hyperedges and the projection of higher-order ones. The objective is to transform the original non-uniform hypergraph into a weighted uniform hypergraph, on which a well-defined H-eigenvector centrality can be computed.

Specifically, let $\mathcal{H} = (V, E, w)$ be a weighted hypergraph, where V is the set of nodes, E is the set of hyperedges, and $w(e)$ denotes the weight of hyperedge e. Let $\mid e \mid$ reflect the size of hyperedge e and let $M = \max_{e \in E} \mid e \mid$ be the maximum order observed in the hypergraph. To compute a spectral centrality measure, a target order p, with $2 \leq p \leq M$, is defined. Then, the procedure transforms all hyperedges so that they have the same size p.

B1. "Uplift" Procedure. This procedure is applied to hyperedges whose size is smaller than the target order, that is, to every hyperedge $e \in E$ such that $|\, e \,| = k < p$. The key idea is to add an auxiliary node, denoted by $\star$, as many times as necessary for the hyperedge to reach size p. Thus, an original hyperedge $e = \{i_1, \dots, i_k\}$ is transformed into:

$$\tilde{e} = \{i_1, \dots, i_k, \underbrace{\star, \dots, \star}_{p-k \text{ times}}\}.$$

The node $\star$ does not belong to the original system, since it is an auxiliary node introduced to allow for the tensor-based uniformization of the hypergraph. Because the adjacency tensor of an undirected hypergraph is symmetric, the introduction of the auxiliary node generates more tensor permutations than those associated with the original hyperedge. For this reason, Contreras-Aso et al. introduce a combinatorial correction factor that avoids overcounting the strength of the original relationship. For a hyperedge of size k increased to order p, the corrected tensor weight can be written as

$$\widetilde{w}(e) = w(e)\frac{(p-k)k!}{p!}.$$

This factor preserves the total contribution of the original hyperedge once tensor symmetrization is taken into account. In the simple case of an edge of size 2 lifted to order 3, the factor is

$$\frac{(3-2)2!}{3!} = \frac{1}{3}$$

which is the example discussed by the authors: an interaction $\{i,j\}$ is transformed into $\{i,j,\star\}$, but each artificially added tensor entry receives weight $1/3$ to avoid introducing spurious connectivity.

Once the uniform hypergraph has been constructed by increasing the size of smaller hyperedges, *H-eigenvector centrality* is computed on the associated tensor. For a p-uniform hypergraph with adjacency tensor $\mathcal{T}$, the H-eigenvector is subject to scaling: if c is a solution, any positive multiple of c is also a solution. Therefore, the centrality of the auxiliary node $\star$ can be formally normalized to $c_\star = 1$. Then, for the empirical analysis, the component associated with the auxiliary node is discarded, and only the centralities of the original nodes in V are maintained. This property is key for making the *uplift* procedure compatible with H-eigenvector centrality in uniform hypergraphs.

B2. Projection Procedure. This procedure is applied to hyperedges whose size is larger than the target order, that is, to every hyperedge $e \in E$ with $|\, e \,| = k > p$. In this case, the original hyperedge is replaced by all its possible sub-hyperedges of size p. Formally, for each e, the set $\mathcal{S}_p(e) = \{s \subset e : |\, s \,| = p\}$ is considered. Therefore, a hyperedge of size k generates $\binom{k}{p}$ projected hyperedges of size p. For example, if $e = \{1,2,3,4\}$ and it is projected to $p = 2$, the six edges $\{1,2\}, \{1,3\}, \{1,4\}, \{2,3\}, \{2,4\}, \{3,4\}$ are obtained. The weighting of the projected hyperedges follows a counting criterion: each sub-hyperedge of size p receives one contribution for each higher-order original hyperedge in which it participates. In the weighted case, this contribution may accumulate the weight $w(e)$ of the original hyperedge. Thus, if several higher-order hyperedges generate the same sub-hyperedge s, the final weight of s is obtained by summing those contributions:

$$\widehat{w}(s) = \sum_{e \in E:\, s \subset e,\, |e| > p} w(e).$$

This criterion generalizes the logic of clique projection: a higher-order interaction is represented through all its lower-order interactions, but without introducing factors that artificially increase its relative participation.

B3. Combination: *Uplifted-Projected* H-Eigenvector Centrality. The full procedure combines both operations. Given a target order p:

$$e \in E \Rightarrow \begin{cases} \textit{uplift} \text{ of } e, & \text{if } \mid e \mid < p \\ e \text{ is preserved}, & \text{if } \mid e \mid = p \\ \text{projection of } e, & \text{if } \mid e \mid > p \end{cases}$$

The result is a weighted p-uniform hypergraph. H-eigenvector centrality is then computed on this transformed hypergraph. The resulting measure is referred to by the authors as p-*Uplifted-Projected H-Eigenvector Centrality* (p-UPHEC). When $p = M$, the procedure is equivalent to lifting all smaller hyperedges to the maximum observed order; in this case, the resulting measure corresponds to m-Uplifted H-Eigenvector Centrality (m-UHEC). When p is lower than M, the procedure combines the projection of larger hyperedges with the *uplift* of smaller ones.

If the original hypergraph is strongly connected, the transformed hypergraph preserves the connectivity required to apply Perron-Frobenius-like associated theorems for nonnegative tensors. Therefore, a positive H-eigenvector centrality exists and is unique (up to scaling). This property allows the resulting vector to be interpreted as a well-defined centrality measure for the original nodes of the hypergraph.

Intuitively, the procedure makes it possible to incorporate information from interactions of different orders simultaneously. Smaller hyperedges are not discarded, but rather lifted through the auxiliary node; larger hyperedges are not eliminated either, but are projected onto the selected order of analysis. In this way, the resulting centrality summarizes the importance of each node within the full structure of the non-uniform hypergraph, avoiding the need to compute separate centralities for each hyperedge order. This is particularly useful in empirical applications where higher-order interactions are heterogeneous, as in financial networks.

Appendix C. Robustness check: amplified systemic impact on traditional bipartite networks

As a robustness exercise, we computed the systemic impact resulting from the distress of the top-ranked financial institutions using the original bipartite network, rather than the hypergraph representation. For this purpose, we applied a DebtRank algorithm adapted to the bipartite setting, analogous to the one presented above for hypergraphs and consistent with the approaches used by Silva et al. (2018) for the Brazilian credit network and by Aoyama et al. (2013) for the Japanese credit network.

Figure 10. **Amplified systemic impact in the bipartite network after shocking the top-ranked financial institutions identified by each centrality metric** (% of total credit in the system)

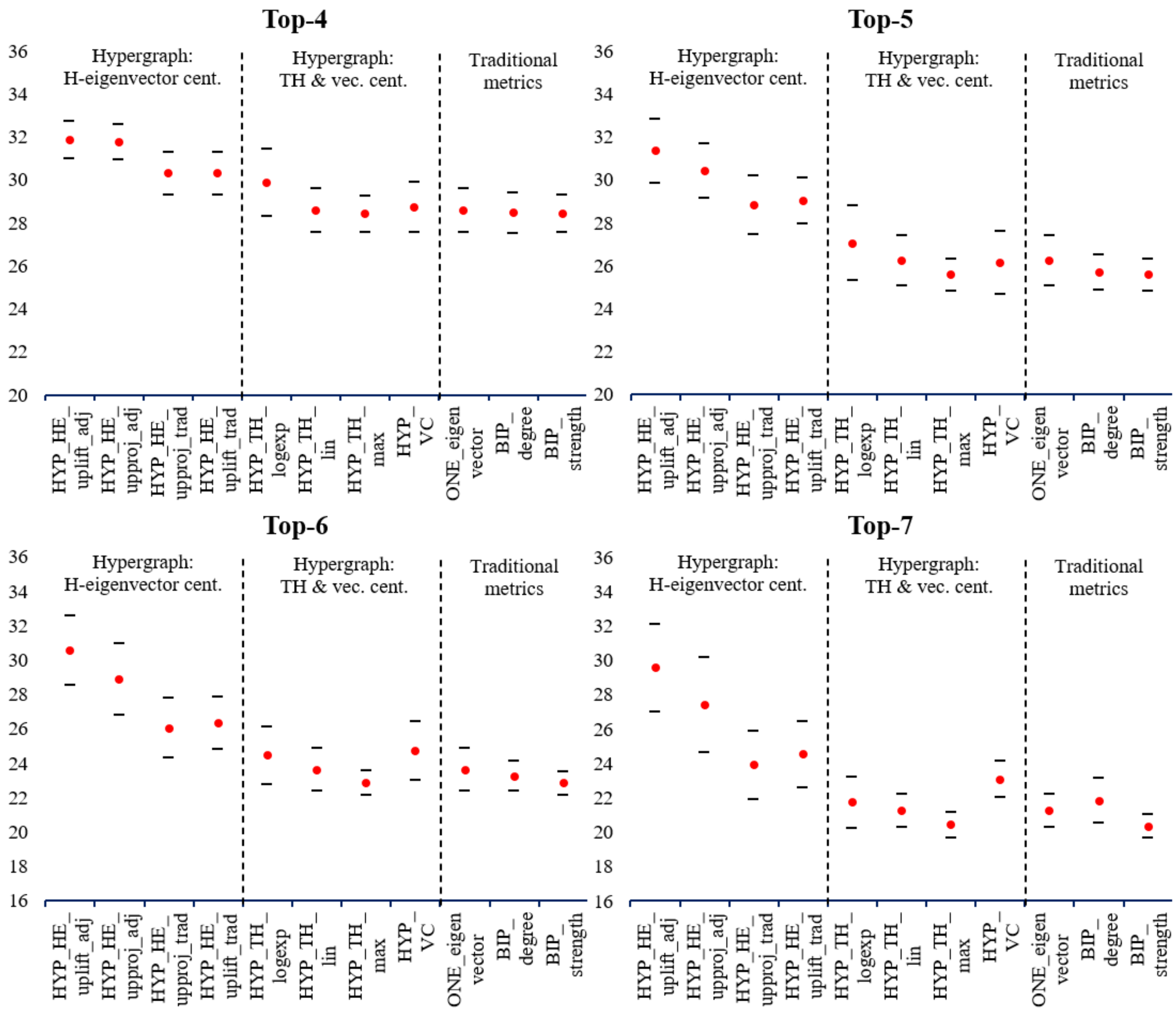

Notes: Each panel shows the average amplified impact across all months under analysis obtained by shocking the top-k financial institutions identified by each centrality measure (for k = 4, 5, 6, and 7), with the resulting distress propagated through the original bipartite network. The black lines indicate a range of ±1 standard deviation. See Table 2 for a summary of the centrality metrics and their abbreviations.

The results (reported in Figure 10) show that both the systemic impact and the relative magnitudes associated with each centrality measure remain virtually identical to those obtained in the main exercise of this paper (Figure 9). This confirms that our conclusions do not depend on the specific adaptation of the DebtRank algorithm to the hypergraph setting. Furthermore, the differences in terms of amplified systemic impact between H-eigenvector centrality measures and traditional metrics also remain statistically significant, as indicated by 95% confidence intervals estimated using a block bootstrap (Table 4).

Table 4. **Differential impact of shocks to top-ranked financial institutions in the bipartite network: traditional metrics versus H-eigenvector centrality measures** (percentage points; 95% confidence intervals in brackets; differences computed as row minus column)

	Shocked top-ranked institutions	**BIP_degree**	**BIP_strength**	**ONE_eigenvector**
HYP_HE_ uplift_adj	**Top-4**	3.41 [2.61, 4.32]	3.46 [2.70, 4.33]	3.31 [2.41, 4.20]
	Top-5	5.66 [4.70, 6.71]	5.77 [4.78, 6.86]	5.12 [3.94, 6.23]
	Top-6	7.31 [6.24, 8.58]	7.73 [6.57, 9.03]	6.93 [5.35, 8.46]
	Top-7	7.71 [6.20, 9.49]	9.21 [7.71, 10.79]	8.30 [6.61, 9.97]
HYP_HE_ upproj_adj	**Top-4**	3.29 [2.58, 4.02]	3.34 [2.68, 4.06]	3.19 [2.43, 3.94]
	Top-5	4.72 [3.99, 5.53]	4.82 [4.12, 5.60]	4.18 [3.19, 5.19]
	Top-6	5.64 [4.40, 7.00]	6.05 [5.10, 7.30]	5.26 [4.14, 6.57]
	Top-7	5.58 [3.94, 7.44]	7.08 [5.72, 8.73]	6.17 [4.81, 7.64]
HYP_HE_ uplift_trad	**Top-4**	1.83 [1.17, 2.53]	1.88 [1.25, 2.59]	1.73 [1.09, 2.45]
	Top-5	3.35 [2.72, 3.93]	3.45 [2.76, 4.04]	2.81 [1.92, 3.63]
	Top-6	3.08 [2.64, 3.78]	3.49 [2.93, 4.16]	2.69 [1.87, 3.45]
	Top-7	2.69 [1.98, 3.75]	4.19 [3.62, 4.91]	3.28 [2.51, 4.11]
HYP_HE_ upproj_trad	**Top-4**	1.84 [1.21, 2.54]	1.89 [1.28, 2.63]	1.74 [1.07, 2.47]
	Top-5	3.13 [2.45, 3.78]	3.24 [2.50, 3.93]	2.59 [1.70, 3.54]
	Top-6	2.81 [2.14, 3.54]	3.22 [2.44, 4.01]	2.42 [1.38, 3.33]
	Top-7	2.06 [1.38, 2.98]	3.56 [2.99, 4.22]	2.65 [1.99, 3.37]

Notes: Each value reflects the average difference (in p.p.) between the amplified systemic impact of shocking the top-k financial institutions identified by the centrality measure shown in the row and the corresponding impact obtained for the top-k financial institutions identified by the centrality measure shown in the column. A 95% confidence interval is reported in brackets, computed through block-bootstrapping, with a block size of 3 to account for potential autocorrelation. The intervals do not change significantly when alternative block sizes are used.

8. References

Accominotti, O., Lucena-Piquero, D., & Ugolini, S. (2023). Intermediaries' substitutability and financial network resilience: A hyperstructure approach. *Journal of Economic Dynamics and Control*, *153*, 104700. https://doi.org/10.1016/j.jedc.2023.104700

Acemoglu, D., Ozdaglar, A., & Tahbaz-Salehi, A. (2015). Systemic Risk and Stability in Financial Networks. *American Economic Review*, *105*(2), 564-608. https://doi.org/10.1257/aer.20130456

Acharya, V. V., Pedersen, L. H., Philippon, T., & Richardson, M. (2017). Measuring Systemic Risk. *The Review of Financial Studies*, *30*(1), 2-47. https://doi.org/10.1093/rfs/hhw088

Adrian, T., & Brunnermeier, M. K. (2016). CoVaR. *American Economic Review*, *106*(7), 1705-1741. https://doi.org/10.1257/aer.20120555

Akgüller, Ö., & Balcı, M. A. (2026). Detecting Financial Contagion Through Higher-Order Networks: A Deep Learning Approach to Emerging Market Risk. *Computational Economics*. https://doi.org/10.1007/s10614-025-11287-3

Alaeddini, M., Madiès, P., Reaidy, P. J., & Dugdale, J. (2023). Interbank money market concerns and actors' strategies—A systematic review of 21st century literature. *Journal of Economic Surveys*, *37*(2), 573-654. https://doi.org/10.1111/joes.12495

Aoyama, H., Battiston, S., & Fujiwara, Y. (2013). *DebtRank Analysis of the Japanese Credit Network*. Research Institute of Economy, Trade and Industry (RIETI). https://EconPapers.repec.org/RePEc:eti:dpaper:13087

Barabási, A.-L. (2016). *Network science*. Cambridge University Press.

Bardoscia, M., Battiston, S., Caccioli, F., & Caldarelli, G. (2015). DebtRank: A Microscopic Foundation for Shock Propagation. *PLOS ONE*, *10*(6), e0130406. https://doi.org/10.1371/journal.pone.0130406

Battiston, F., Cencetti, G., Iacopini, I., Latora, V., Lucas, M., Patania, A., Young, J.-G., & Petri, G. (2020). Networks beyond pairwise interactions: Structure and dynamics. *Physics Reports*, *874*, 1-92. https://doi.org/10.1016/j.physrep.2020.05.004

Battiston, S., Puliga, M., Kaushik, R., Tasca, P., & Caldarelli, G. (2012). DebtRank: Too Central to Fail? Financial Networks, the FED and Systemic Risk. *Scientific Reports*, *2*(1), 541. https://doi.org/10.1038/srep00541

BCBS. (2024). *Global systemically important banks: Revised assessment framework*. Consultative Document, Bank for International Settlements.

Benson, A. R. (2019). Three Hypergraph Eigenvector Centralities. *SIAM Journal on Mathematics of Data Science*, *1*(2), 293-312. https://doi.org/10.1137/18M1203031

Bianconi, G. (2021). *Higher-Order Networks*. Cambridge University Press. Cambridge Core. https://doi.org/10.1017/9781108770996

Cao, J., Wen, F., Stanley, H. E., & Wang, X. (2021). Multilayer financial networks and systemic importance: Evidence from China. *International Review of Financial Analysis*, *78*, 101882. https://doi.org/10.1016/j.irfa.2021.101882

Chun, J., Bu, F., Kim, Y., Miyauchi, A., Bonchi, F., & Shin, K. (2025). A Survey on Centrality and Importance Measures in Hypergraphs: Categorization and Empirical Insights. *ArXiv*, *abs/2512.00107*. https://api.semanticscholar.org/CorpusID:283450711

Contreras-Aso, G., Pérez-Corral, C., & Romance, M. (2024). Uplifting edges in higher-order networks: Spectral centralities for non-uniform hypergraphs. *AIMS Mathematics*, *9*(11), 32045-32075. https://doi.org/10.3934/math.20241539

De Masi, G., Fujiwara, Y., Gallegati, M., Greenwald, B., & Stiglitz, J. E. (2011). An Analysis of the Japanese Credit Network. *Evolutionary and Institutional Economics Review*, *7*(2), 209-232. https://doi.org/10.14441/eier.7.209

De Masi, G., & Gallegati, M. (2012). Bank-firms topology in Italy. *Empirical Economics*, *43*(2), 851-866. https://doi.org/10.1007/s00181-011-0512-x

Elosegui, P., Forte, F. D., & Montes-Rojas, G. (2022). Network structure and fragmentation of the Argentinean interbank markets. *Latin American Journal of Central Banking*, *3*(3), 100066. https://doi.org/10.1016/j.latcb.2022.100066

Fang, L., Zhao, T., Yu, J., Guo, Q., Li, X., & Zhang, C. (2025). TD-HCN: A trend-driven hypergraph convolutional network for stock return prediction. *Neural Networks*, *190*, 107729. https://doi.org/10.1016/j.neunet.2025.107729

Forte, F. D. (2020). Network topology of the Argentine interbank money market. *Journal of Complex Networks*, *8*(4). https://doi.org/10.1093/comnet/cnaa039

FSB-IMF-BIS. (2009). *Guidance to Assess the Systemic Importance of Financial Institutions, Markets and Instruments: Initial Considerations*. G20 Finance Ministers and Governors.

Fujiwara, Y., Aoyama, H., Ikeda, Y., Iyetomi, H., & Souma, W. (2009). *Structure and Temporal Change of the Credit Network between Banks and Large Firms in Japan*. *Economics*, *3*(1). https://doi.org/10.5018/economics-ejournal.ja.2009-7

Haldane, A. (2009). *Rethinking the financial network*. Speech given at the Financial Student Association, Amsterdam.

Han, H., Xie, L., Chen, S., & Xu, H. (2023). Stock trend prediction based on industry relationships driven hypergraph attention networks. *Applied Intelligence*, *53*(23), 29448-29464. https://doi.org/10.1007/s10489-023-05035-z

Hüser, A.-C. (2015). Too interconnected to fail: A survey of the interbank networks literature. *Journal of Network Theory in Finance*, *1*(3), 1-50. https://doi.org/10.2139/ssrn.2577241

Iacopini, I., Karsai, M., & Barrat, A. (2024). The temporal dynamics of group interactions in higher-order social networks. *Nature Communications*, *15*(1), 7391. https://doi.org/10.1038/s41467-024-50918-5

Kovalenko, K., Romance, M., Vasilyeva, E., Aleja, D., Criado, R., Musatov, D., Raigorodskii, A. M., Flores, J., Samoylenko, I., Alfaro-Bittner, K., Perc, M., & Boccaletti, S. (2022). Vector centrality in hypergraphs. *Chaos, Solitons & Fractals*, *162*, 112397. https://doi.org/10.1016/j.chaos.2022.112397

Lei, J., Shen, P., & Li, Z. (2025). Multilayer bank-firm networks and financial risk contagion. *Physica A: Statistical Mechanics and its Applications*, *675*, 130838. https://doi.org/10.1016/j.physa.2025.130838

Li, B., & Zhang, X. (2024). Systemic risk and financial networks. *The Quarterly Review of Economics and Finance*, *94*, 25-36. https://doi.org/10.1016/j.qref.2023.12.012

Lind, P. G., González, M. C., & Herrmann, H. J. (2005). Cycles and clustering in bipartite networks. *Physical Review E*, *72*(5), 056127. https://doi.org/10.1103/PhysRevE.72.056127

Liu, Y., Sadiq, M., Wen, F., & Cao, Z. (2024). Interbank deposits and bank systemic risk. *International Review of Financial Analysis*, *96*, 103718. https://doi.org/10.1016/j.irfa.2024.103718

Luu, D. T., & Lux, T. (2018). Identifying patterns in the bank-sector credit network of Spain. *Journal of Network Theory in Finance*, *4*(1), 1-38. https://doi.org/10.21314/JNTF.2018.037

Marotta, L., Miccichè, S., Fujiwara, Y., Iyetomi, H., Aoyama, H., Gallegati, M., & Mantegna, R. N. (2015). Bank-Firm Credit Network in Japan: An Analysis of a Bipartite Network. *PLOS ONE*, *10*(5), e0123079. https://doi.org/10.1371/journal.pone.0123079

Martinez-Jaramillo, S., Carmona, C., & Kenett, D. (2019). Interconnectedness and financial stability. *Journal of Risk Management in Financial Institutions*, *12*(2). https://doi.org/10.69554/OTBZ2655

Miranda, R., & Tabak, B. (2013). *Contagion Risk within Firm-Bank Bivariate Networks* [Working Papers Series]. Central Bank of Brazil, Research Department.

Newman, M. (2010). *Networks: An Introduction*. Oxford University Press. https://doi.org/10.1093/acprof:oso/9780199206650.001.0001

Patania, A., Petri, G., & Vaccarino, F. (2017). The shape of collaborations. *EPJ Data Science*, *6*(1), 18. https://doi.org/10.1140/epjds/s13688-017-0114-8

Qi, L., & Luo, Z. (2017). *Tensor analysis: Spectral theory and special tensors*. Society for Industrial and Applied Mathematics.

Silva, T. C., Alexandre, M. da S., & Tabak, B. M. (2018). Bank lending and systemic risk: A financial-real sector network approach with feedback. *Journal of Financial Stability*, *38*, 98-118. https://doi.org/10.1016/j.jfs.2017.08.006

Straka, M. J., Caldarelli, G., Squartini, T., & Saracco, F. (2018). From Ecology to Finance (and Back?): A Review on Entropy-Based Null Models for the Analysis of Bipartite Networks. *Journal of Statistical Physics*, *173*(3), 1252-1285. https://doi.org/10.1007/s10955-018-2039-4

Sulas, A., Maringer, D., & Paterlini, S. (2025). Systemic risk from overlapping portfolios: A multi-objective optimization framework. *International Review of Financial Analysis*, *97*, 103794. https://doi.org/10.1016/j.irfa.2024.103794

Traversa, P., Ferraz de Arruda, G., Vazquez, A., & Moreno, Y. (2023). Robustness and Complexity of Directed and Weighted Metabolic Hypergraphs. *Entropy*, *25*(11), 1537. https://doi.org/10.3390/e25111537

Tudisco, F., & Higham, D. J. (2021). Node and edge nonlinear eigenvector centrality for hypergraphs. *Communications Physics*, *4*(1), 201. https://doi.org/10.1038/s42005-021-00704-2

Wang, G., Zhao, H., Shu, L., & Song, L. (2025). Understanding risk spillover in multi-layer financial networks: The role of bank–firm connections. *International Review of Financial Analysis*, *105*, 104404. https://doi.org/10.1016/j.irfa.2025.104404